INL/CON-25-83236-Revision-0

Advanced Manufactured Strain Sensors for Extreme Environments

June 2025

Timothy Le Phero, Amey Rajendra Khanolkar, James A Smith, Michael D McMurtrey, Brian J. Jaques, David Estrada

Changing the World's Energy Future

Idaho National Laboratory

INL is a U.S. Department of Energy National Laboratory operated by Battelle Energy Alliance, LLC

INL/CON-25-83236-Revision-0

Advanced Manufactured Strain Sensors for Extreme Environments

Timothy Le Phero, Amey Rajendra Khanolkar, James A Smith, Michael D McMurtrey, Brian J. Jaques, David Estrada

June 2025

Idaho National Laboratory
Idaho Falls, Idaho 83415

http://www.inl.gov

Prepared for the
U.S. Department of Energy
Under DOE Idaho Operations Office
Contract DE-AC07-05ID14517

Advanced Manufactured Strain Sensors for Extreme Environments

Timothy L. Phero[1,2,3], Amey R. Khanlokar[2], James A. Smith[2], Michael D. McMurtrey[2], David Estrada[1,2,3], and Brian J. Jaques[1,3]

[1]Micron School of Materials Science and Engineering, Boise State University, Boise, ID
[2] Idaho National Laboratory, Idaho Falls, ID
[3] Center for Advanced Energy Studies, Idaho Falls, ID

[leave space for DOI, which will be inserted by ANS]

ABSTRACT

Experimentation at irradiation test facilities are essential for reducing the innovation time of developmental fuels, fuel cladding, and structural materials employed in next-generation nuclear reactors. However, due to the harsh conditions generated in such reactors and limited instrumentation space, the evaluation of a material's mechanical properties is often limited to characterization after the materials have been removed from reactor conditions, or post-irradiation examination. These experiments are costly, time-consuming, and fail to capture the critical time-evolving phenomena that occur during the irradiation experiments. Advanced manufactured digital image correlation patterns and strain sensor devices serve as two promising technologies that can be deployed in the confined and challenging orientations of these irradiation experiments while also providing key insight on salient materials phenomena (i.e., mechanical properties).To guide the development of the printed strain sensors prior to their deployment in critical experiments, the adhesion strength between the substrate and printed film interface is measured via tensile testing and a non-contact laser-induced spallation technique. The establishment of these process control steps helped guide the successful fabrication and testing of direct-write strain sensing devices discussed in this work. The fabrication process controls are necessary for enabling the sustained operation of these strain sensing device through experimentation and minimize the potential for premature failure.

Keywords: Adhesion test, qualification, strain gauge, additive manufacturing

1. INTRODUCTION

The development of non-invasive, real-time monitoring techniques that measure salient materials properties is essential towards advancements in nuclear energy technologies. To expand the structural health monitoring capabilities at irradiation test facilities, additively manufactured (AM) strain sensing devices has become of interest as a viable technology to fill the design space where specialized requirements are important (e.g., environmental conditions, space limitation, materials interaction). The application of direct-write AM provides has opportunities to offset the limitations of traditional manufacturing by allowing the fabrication of sensing devices with designs and materials that can be tailored and rapidly prototyped to fit the needed size limitation and materials compatibility for any specific application. This enables the exploration and fabrication of specialized nuclear sensing devices that were rendered economically non-viable for large scale production by commercial vendors [1].

To mitigate premature failure and enable the successful sustained operation of AM sensors, the use of qualification tests can be used as an intermediate process control step to verify the robustness and reliability of the sensors before they are deployed in experiments. Non-contact techniques, such as laser-induced spelling, are quick and can be easily integrated in a roll-to-roll manufacturing scheme. The ability to

characterize the adhesion strength of these AM sensors during fabrication would prevent value-added processing to defective products and lead towards the standardization of printed AM films on substrate materials. This work discusses the use of adhesion qualification testing as a viable technique for down-selecting materials and/or qualifying the robustness of the materials-interface. Printed strain gauges and DIC patterns [2] provides crucial real-time validation metrics for both developmental strain sensing technologies and modeling/simulation efforts for the development of accurate digital twins.

For the strain gauges, the materials system of interest in this work is silver and barium strontium titanium oxide (BST) films on stainless steel 316L (SS316L) substrate. Silver is a readily available commercial ink and serves as the conducting electrode material for the strain gauge. Due to BST's high dielectric constant and tunable dielectric properties [3], there is also an interest for its application as an insulation/encapsulation layer for capacitive strain gauges (CSG) and contrasting DIC pattern when printed on structural materials. In this work, we discuss the development of a qualification process that will help determine and address any challenges (i.e., mechanical failure of thick prints) of the AM sensor prior to its application in experimental tests. To demonstrate the qualification process in this report, both laser spallation and uniaxial tensile tests using dynamic and quasi-static loading, respectively, will be discussed. This work guided the fabrication of CSGs on SS316L and helps increase the efficacy of printed strain sensors used in extreme environments.

2. METHODS

2.1. Fabrication of Strain Gauge

For this work, the strain gauges were fabricated using a silver nanoparticle ink (JS-A21AE, Metalon) and a barium strontium titanium oxide (BST) nanoparticle ink insulating/encapsulating dielectric on a SS316L tensile specimen. AJP was selected as the AM method for fabrication since it can fabricate small form factor devices with a wide variety of ink materials and substrate geometries. The AJP printing process parameters used to print the BST are listed in Table I. The BST layer is sintered at 600 °C for 3-hours in a benchtop muffle furnace in air (Thermo Scientific Thermolyne) with a heating/cooling rate of 2 °C/min. After curing the BST layer, the silver IDE CSG is fabricated on top of the BST insulating layer using the printing process parameters for silver in Table . The silver strain gauges were sintered at 200 °C for 1-hours in the benchtop muffle furnace with a heating/cooling rate of 2 °C/min.

Table I. Barium Strontium Titanate and Silver Ink Printing Parameters

Parameter	BST	Silver
Nozzle diameter (μm)	300	150
Aerosol Jet Atomizer type	Pneumatic	Ultrasonic
Carrier/Atomizer gas flow rate (sccm)	700	27
Exhaust flow rate (sccm)	630	-
Sheath gas flow rate (sccm)	40	57
Number of passes	1	2
Standoff distance (mm)	3	3
Platen temperature (°C)	70	60
Water chiller temperature (°C)	-	20
Ultrasonic atomizer power (amp)	-	0.50
Printing speed (mm/s)	6	4

2.2. Laser Spallation

To test the adhesion of the AM silver and BST films, a laser-induced spallation technique was used. As shown in Figure 1, the AM films were printed to have a dimension of 5 mm × 5 mm on stainless steel 316L substrates. The average thickness of the BST films had a range between ≈0.9 µm to ≈8.5 µm. Figure 2(a) shows a schematic representation of the laser-induced spallation technique. High energy laser pulses derived from the generation laser impinge the sample on the laser energy-absorbing black tape through the clear PVC laser energy-confining film. Rapid thermoelastic expansion of the black absorbing layer due to confinement generates a high amplitude compressive stress wave that propagates through the substrate. After reflection at the free surface of the printed pad on the opposite side of the SS316 substrate, the stress wave loads the film-substrate interface in tension. Figure 2(b) illustrates the loading mechanism by the propagating stress wave in the laser-induced spallation experiment. For one-dimensional wave idealization adopted in the calculation of the film-substrate interfacial stress, the generation-pulsed laser beam was focused to a 3 mm diameter spot, which is approximately three times the substrate thickness [4, 5]

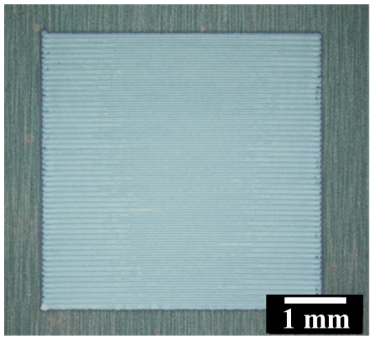

Figure 1. Optical image of a barium strontium titanium oxide film printed on SS316 substrate for laser-induced spallation testing.

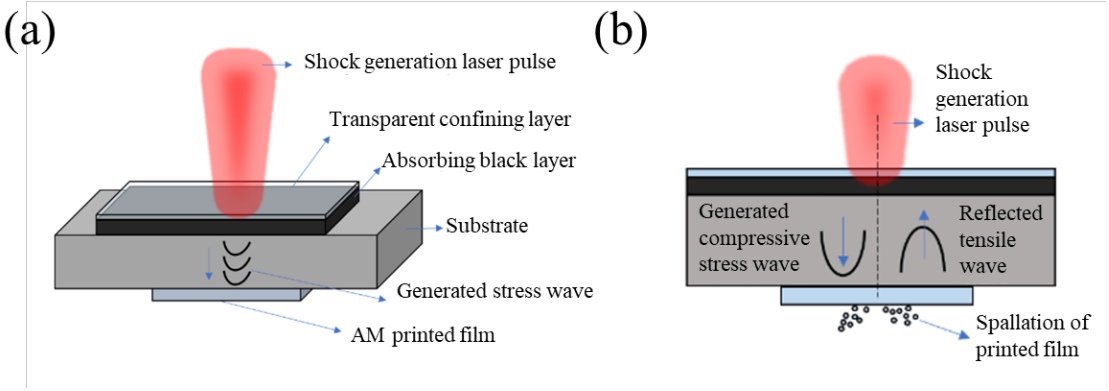

Figure 2. (a) Schematic representation of the experimental geometry of the laser-induced spallation technique. (b) Illustration of the spallation/fracture of the printed film by the laser-generated shock wave.

2.3. Mechanical Testing

Figure 3(a) shows the sample that was fabricated within the gauge length of a SS316L tensile specimen for the quasi-static strain testing. Five 1.5 mm x 12 mm (L x W) rectangular films were fabricated with varying thickness to investigate the mechanical robustness of the films with mechanical loading. Shown in Figure

3(b) is the thickness/height profile of each of the five pads using a stylus profilometer. Samples 1, 2, 3, 4, and 5 have an average thickness of 2.6 µm, 6.2 µm, 10.1 µm, 16.0 µm, and 3.9 µm, respectively. Each sample was printed with varying layers to increase the film thickness since AM deposition of a specific film thickness is difficult, if not impossible, to achieve consistently.

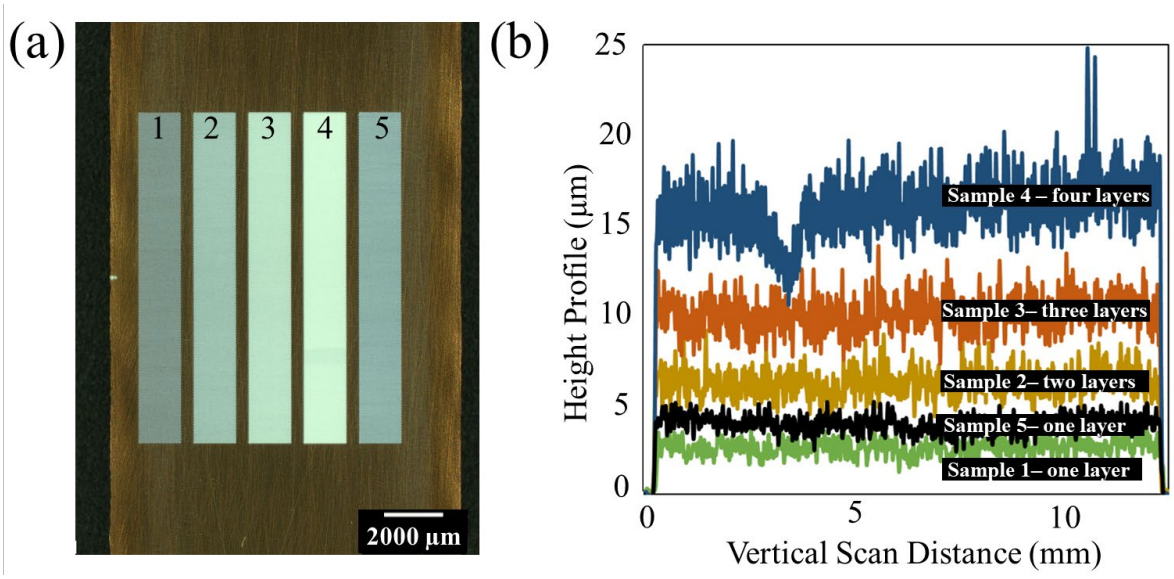

Figure 3. (a) shows the sample that were fabricated for the quasi-static strain testing. Each rectangular pad is 12 mm x 1.5 mm (L x W) and was printed sequentially from left to right. Sample 1, 2, 3, 4, and 5 were printed with one, two, three, four, and one layer of barium strontium titanate. (b) Using a profilometry, the average thickness of samples 1, 2, 3, 4, and 5 are 2.6 µm, 6.2 µm, 10.1 µm, 16.0 µm, and 3.9 µm, respectively.

Figure 4 shows the sample loaded in a uniaxial mechanical test fixture with a calibrated extensometer for strain measurement. A digital single-lens reflex camera outfitted with a lens used for macro photography was used to image the sample throughout the test. The sample was continuously pulled in tension at a rate of 0.3 mm/s to failure at room temperature. The test was paused at various strains to allow time for the image to be captured.

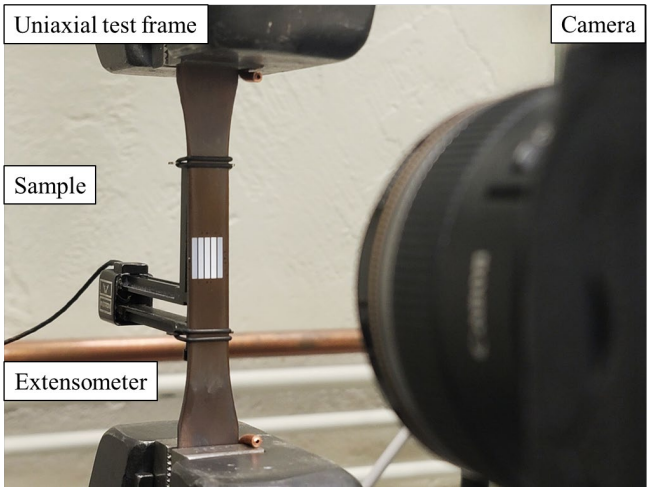

Figure 4. The quasi-static test was performed in a uniaxial test frame with an attached and calibrated extensometer up to 10% strain. A camera with a macro lens was used to image the sample periodically throughout the test.

3. RESULTS

3.1 Mechanical Testing

Figure 5 shows that there was no visibly observed cracking or delamination in the films when mechanically strained within the linear elastic region of SS316L (i.e., up to ≈0.1% strain). This is where the majority of the testing for qualifying the gauge factor and overall performance of the printed capacitive strain gauges are conducted. The surfaces of all five samples remained unchanged with no signs of failure up to 1.0% strain. As shown in Figure 5, cracks began forming on the surfaces of the films at approximately 5.0% strain. Note that the periodic dips in stress were when the test was paused to allow the camera to take an image. These cracks are more visible in the images at 7.5% strain. At 10.0% strain, large sections of the thickest BST film (i.e., Sample 4) delaminated from the substrate. Beyond 10.0% strain, the extensometer was removed to prevent damaging the hardware. Crosshead displacement was used to calculate the strain in the tensile sample after removing the extensometer. Shown in Figure 6, the next sample to have observable delamination was Sample 3 at 30% strain and followed by Sample 5. Sample 1 and Sample 2 did not experience the same level of delamination at these high strain levels. It was observed that the necking of the SS316L tensile specimen was not in the middle of the reduced gage section of the substrate but rather near the shoulder of the reduced gage section of the tensile specimen. This may have caused non-uniform stresses/strain within the reduced gage section of the tensile specimen at the high plastic strains tested. The difference in fracture morphology of Sample 1 and 5, despite having similar film thicknesses, could be caused by a combination of factors including, but not limited to: localized strain, stochastic failure of ceramics, substrate/sample preparation. For the BST/SS316L system, these results show that mechanical stress will not cause cracking and/or debonding of the film when testing in the linear elastic region of SS316L at room temperature. The test for determining the sensitivity of the strain gauges printed on BST are within the linear elastic region of SS316L at room temperature and elevated temperatures > 300 °C. These mechanical tests require a longer preparation time and will be paired with the laser-based technique, discussed in the next section, to allow for redundancy and quicker sensor qualification testing.

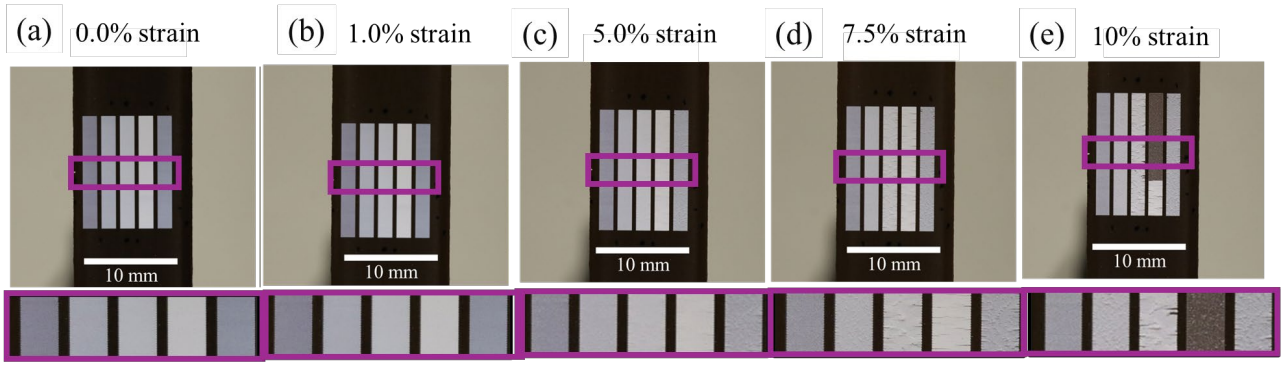

Figure 5. Macro-images of the barium strontium titanate sample under mechanical, quasi-static strains between 0% strain and 10% strain when tested at room temperature. There was no visible cracking, delamination or change in the topography of the film in the elastic region of the SS316L (i.e., under 1.0% strain). The topography of all five samples had varying levels of cracking, which becomes noticeable at 5.0% strain. The thickest sample (i.e., sample 4 with four printed layers of BST), was the first sample to fully delaminate at 10% strain.

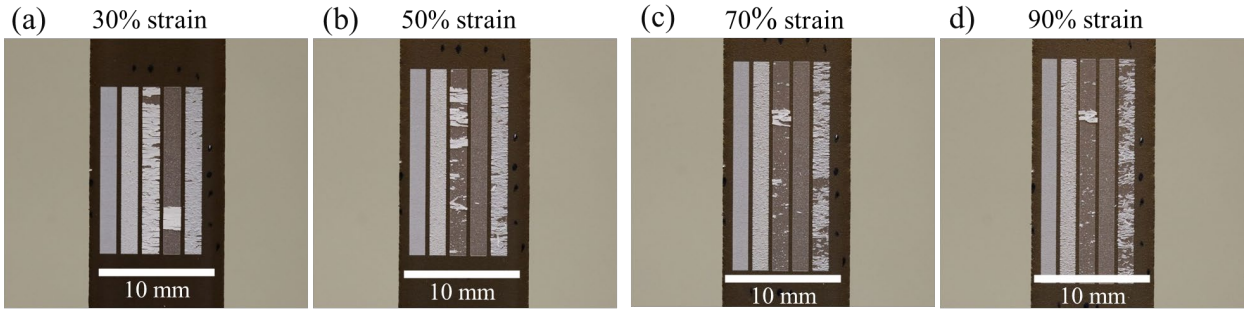

Figure 6. Macro-images of the barium strontium titanate sample under mechanical, quasi-static strains between 30% strain and 90% strain when tested at room temperature.

3.2 Laser-Induced Spallation of BST and Silver

Laser-induced spallation of the BST film in this study was conducted using the Laser Shock System (LSS) at Idaho National Laboratory [4]. This technique uses a pulsed laser to generate an ultrasonic shock wave in the substrate, which loads the film-substrate interface in tension at high strain rates. Shown in Figure 7 are optical images of three BST samples with thicknesses between 1.8 – 2.9 μm. After shocking the films, it was observed that all three samples had similar fracture morphologies when subject to laser-generated stress waves at the lowest laser energy of 180 mJ. These films exhibited a mixture of failure modes (e.g., intralayer failure of BST film and interlayer failure at film/substrate interface) that entails a partial ejection of the BST film from the substrate. To further investigate the effect of film thickness with interface strength, Figure 8 shows the peak surface velocity measurements when there was indication of failure of the BST sample. There is a significant amount of scatter in the resulting data in Figure 8 due to the expected stochastic fracture/ failure of BST. By taking the average of the data (square marker), a trend can be identified that shows thinner films can support more stress. The laser spallation results show that there is a higher surface velocity just prior to film/substrate interface failure for pad thicknesses at less than ≈3.0 μm. The higher surface velocities just prior to interface failure indicates the higher resilience of thinner BST prints when subjected to stress waves at high strain rates. Figure 9 shows two sets of BST films that have two different thicknesses that are within these two regions: 1) average film thickness of ≈8 μm and 2) average of film thickness of ≈1.5 μm. The 8 μm thick film had a brittle fracture morphology and failed at the film/ substrate interface after laser shock. Similar to the films observed in Figure 7, the film with the average film thickness of ≈1.5 μm exhibited a mixture of failure modes that includes both within the BST film itself and interlayer failure at the film/ substrate interface.

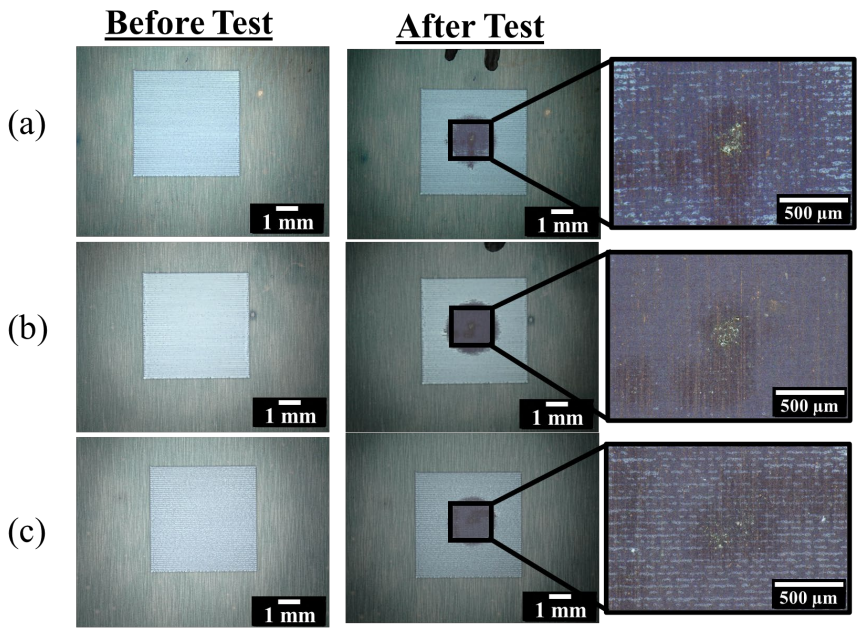

Figure 7. Three samples that were laser shocked at the same 0.18 J laser power. Sample (a), (b) and (c) have film thicknesses 2.1 µm, 2.9 µm, and 1.8 µm, respectively.

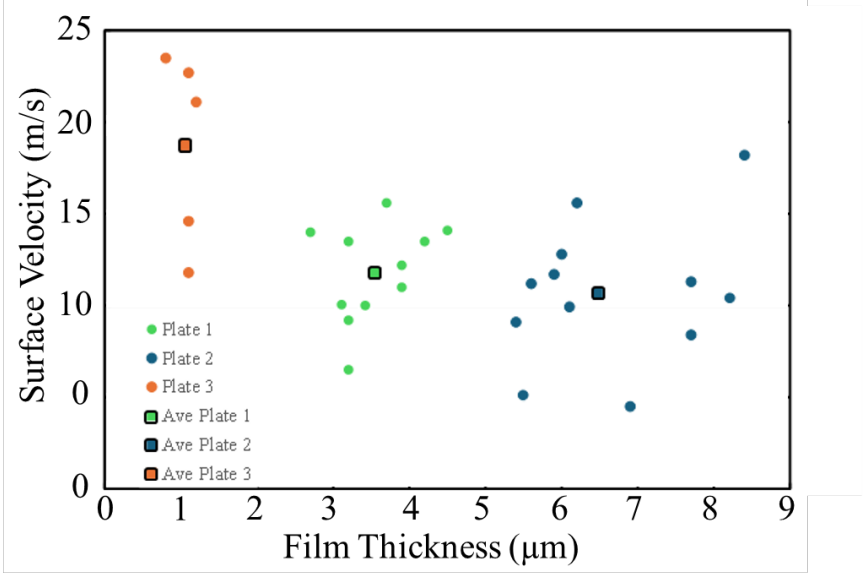

Figure 8. The possible effect of barium strontium titanate (BST) film thickness on the laser energy/ peak surface velocity required to de-bond BST from SS316L.

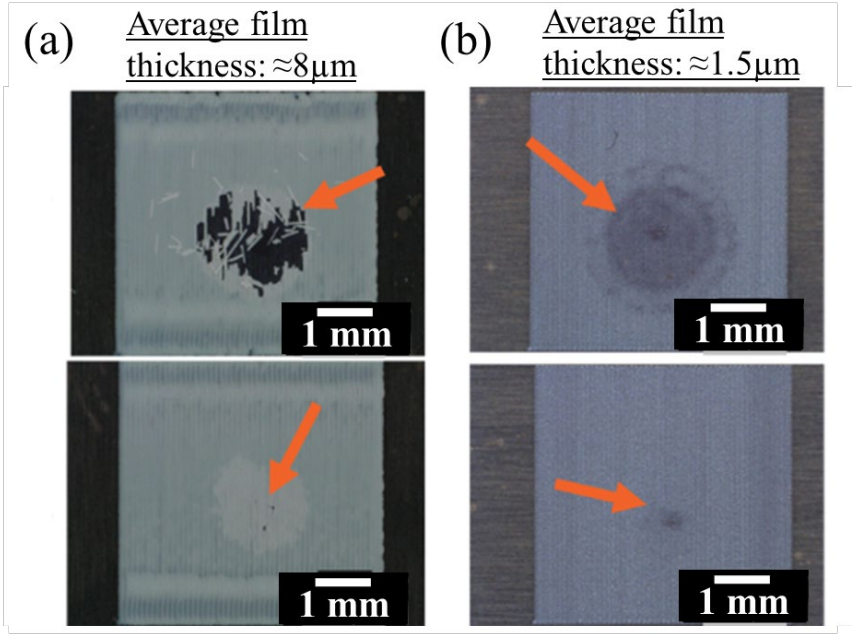

Figure 9. BST films that have been shocked using the laser-spallation. Samples that had average film thicknesses of approximately 8 µm exhibited a brittle fracture at the film/substrate interface. Films with average film thicknesses of approximately 1.5 µm exhibited cohesive, intralayer failure.

3.3 Printed Strain Gauge with BST and Silver

To increase the operating temperature of the CSGs above 300 °C, BST was investigated as a viable insulation/encapsulation material since it has been shown to have a changing dielectric permittivity (i.e., dielectric constant) with strain [6]. The CSGs were initially fabricated with only a BST insulation layer between the printed device and SS316L substrate, as shown in Figure 10, however initial results showed that the CSG had low sensitivity (i.e., gauge factor) to mechanical strain. CSGs were then fabricated with an encapsulation of BST over the CSG. Figure 11 shows the performance of the CSG with and without encapsulation when strained up to 0.11% tensile strain. In Figure 11, the peak tensile strain (i.e., 0.11% tensile strain) during testing is shown as circular symbol. The square symbols show locations of when the CSGs are unloaded and near 0.0% strain. For both encapsulated and unencapsulated CSGs, two noticeable differences are: 1) the magnitudes of the capacitance and 2) the direction of capacitance change while at 0.0% strain and at peak tensile strain (i.e., 0.11% strain). For the unencapsulated CSG, the capacitance decreases with increase in strain which could indicate that the primary mechanism for capacitance change is the increase in gap spacing between the interdigitated electrodes with strain. As shown in Figure 11(b), the difference in capacitance between 0.0% strain and 0.11% strain for CSGs without encapsulation is ≈0.00011, which is a gauge factor of approximately 0.1. For the encapsulated CSG, the capacitance increases with increase in strain which could indicate that the primary mechanism for capacitance change is the increase in dielectric constant of the BST with strain. As shown in Figure 11(b), the difference in capacitance between 0.0% strain and 0.11% strain for CSGs with encapsulation is ≈0.003, which is a gauge factor of approximately 3.6.

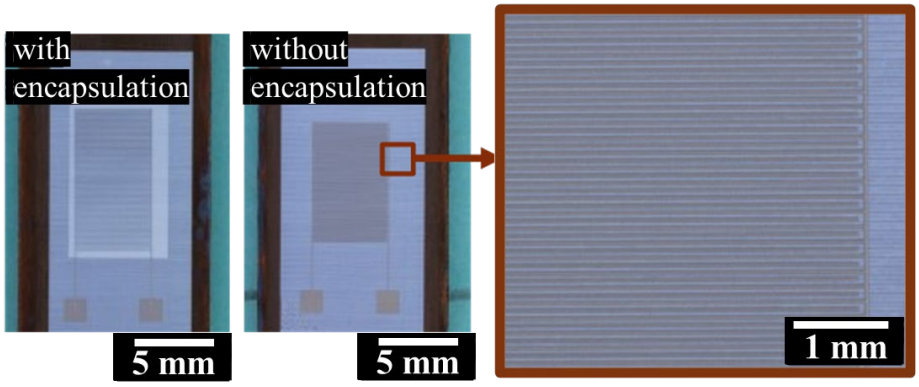

Figure 10. Capacitive strain gauge fabricated with and without an encapsulation layer of barium strontium titanium oxide.

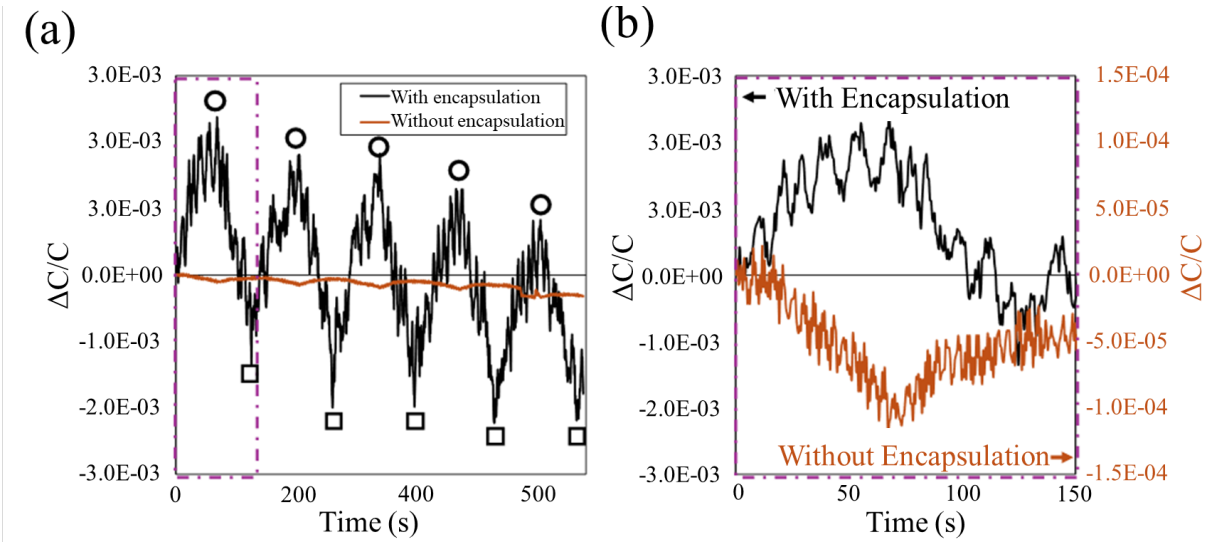

Figure 11. (a) The performance of a capacitive strain gauge with and without an encapsulation layer for five cycles up to 0.11% tensile strain. (b) Shows the zoomed-up region of the first cycle of the test as shown by the dashed region in (a).

4. CONCLUSIONS

Adhesion testing using laser spallation has potential to provide vital feedback on the resilience of the printed layers that can aid the successful deployment of AM sensor devices. Depending on the experimental needs of the sensor, the trends from mechanical testing showed that AM printed BST of various thicknesses between 2.6 µm and 16.0 µm on SS316L at room temperature does not crack and/or delaminate within the elastic region of the substrate. Cracking and delamination of the BST film occurred, however, at higher strains above 5.0%, which is well into the plastic deformation regime of the SS316L specimen. Current testing of strain gauges that use the BST film are within the elastic limit of SS316L. Laser spallation testing showed that the BST films with thicknesses below 3 µm required a higher laser pulse energy to initiate failure/ debonding of the film when loaded with a laser-generated ultrasonic stress wave at high strain rate. Films greater than 3 µm thick were prone had a more brittle fracture morphology when compared to films thinner than 3 µm when shocked with the same laser power. This variability in failure modalities of the BST films under quasi-static loading was also observed in Sample 1 (whose thickness was 2.6 µm) and

Sample 5 (whose thickness was 3.9 μm) in Figure 5 - Figure 6. For silver, sintering temperature was found to be a more dominant variable, with an increase of 102% in the required laser pulse energy required to induced failure for samples sintered at 400°C for 60 min. over those sintered at 200°C for 30 min. Testing of capacitive strain gauge with BST insulation and encapsulation at room temperature had a larger sensitivity to strain (i.e., gauge factor of 3.6) when compared to: 1) capacitive strain gauge without the BST encapsulation and 2) capacitive strain gauge that were previously fabricated with polyimide insulation/ encapsulation [7]. The results discussed in this work enable the fabrication of printed strain gauges that can withstand the extreme environmental conditions of nuclear reactors. Advancements in qualification testing will enable more robust and reliable electronics for in-pile sensing and monitoring using AM devices.

ACKNOWLEDGMENTS

This work was prepared as an account of work sponsored by the U.S. Department of Energy, Office of Nuclear Energy Advanced Sensors and Instrumentation program under DOE Contract DE- AC07-05ID14517. Neither the U.S. Government nor any agency thereof, nor any of their employees, makes any warranty, expressed or implied, or assumes any legal liability or responsibility for the accuracy, completeness, or usefulness, of any information, apparatus, product, or process disclosed, or represents that its use would not infringe privately owned rights. References herein to any specific commercial product, process, or service by trade name, trademark, manufacturer, or otherwise, does not necessarily constitute or imply its endorsement, recommendation, or favoring by the U.S. Government or any agency thereof. The views and opinions of authors expressed herein do not necessarily state or reflect those of the U.S. Government or any agency thereof.

REFERENCES

1. D. S. Engstrom, B. Porter, M. Pacios, H. Bhaskaran, “Additive nanomanufacturing–A review,” *J Mater Res*, **29** (2014) 1792-816.
2. T. L. Phero, K. A. Novich, K. T. Fujimoto, A. R. Khanolkar, B. C. Johnson, M. D. McMurtrey, et al., “Additively Manufactured Strain Sensing for Nuclear Reactor Applications,” *Nuclear Plant Instrumentation, Control, and Human Interface Technologies (NPIC-HMIT) 2023 conference proceedings*, (2023).
3. P. Joshi, M. Cole, “Mg-doped Ba 0.6 Sr 0.4 TiO 3 thin films for tunable microwave applications,” *Appl Phys Lett*, **77** (2000) 289-91.
4. J. Smith, C. Scott, B. Benefiel, B. Rabin, “Interface characterization within a nuclear fuel plate,” Applied *Sciences*, **9** (2019) 249.
5. J. Wang, R.L. Weaver, N.R. Sottos, “A parametric study of laser induced thin film spallation,” *Experimental Mechanics*, **42** (2002) 74-83.
6. [7] T. Shaw, Z. Suo, M. Huang, E. Liniger, R. Laibowitz, J. Baniecki, “The effect of stress on the dielectric properties of barium strontium titanate thin films,” *Appl Phys Lett*, **75** (1999) 2129-31.
7. T. L. Phero, K. A. Novich, B. C. Johnson, M. D. McMurtrey, D. Estrada, B. J. Jaques, “Additively manufactured strain sensors for in-pile applications,” *Sensors and Actuators A: Physical*, **344** (2022) 113691.